Supplementary Information

Expedient Alkyne Semi-Hydrogenation by Using a Bimetallic AgCu-C_3N_4 Single Atom Catalyst

Jingting Song,[‡] Xiangbin Cai,[‡] Zhongxin Chen, Tie Wang, Shibo Xi, Hu Qikun, Ning Yan, and Kian Ping Loh[*]

[#] These authors contributed equally to this work. Correspondence and requests for materials should be addressed to K. P. Loh (*chmlohkp@nus.edu.sg*)

Computational Section:

The calculations were carried out using density functional theory with the revised version of Perdew-Burke-Ernzerhof (revPBE), which can estimate the adsorption of species well.[1-4] The Vienna *ab-initio* simulation package (VASP)[5-8] was employed. The Brillouin zone was sampled only at the Gamma point. The plane wave energy cutoff was set as 400 eV. The Fermi scheme was employed for electron occupancy with an energy smearing of 0.1 eV. The energy (converged to 1.0×10^{-4} eV $atom^{-1}$) and force (converged to 0.06 eV $Å^{-1}$) were set as the convergence criterion for geometry optimization. The spin polarization was considered in all calculations. To accurately describe the van der Waals (vdW), the non-local van der Waals density functional (vdW-DF) was employed.[9,10] The projected Crystal Orbital Hamilton Population (pCOHP) method was used to visualize and analyze chemical bonding between catalysts and adsorbates with an MP-centered k-point of 2 × 2 × 2, and the computer program Local Orbital Basis Suite Toward Electronic-Structure Reconstruction (LOBSTER) was used to process the pCOHP calculation results.[11-12]

Models

A monolayer of 2 × 2 supercell of tri-s-triazine-based *g*-C_3N_4 with periodical boundary conditions was employed as the M-C_3N_4 catalyst model. Meanwhile the differerntal charge of the AgCu-C_3N_4 is investigated. The vacuum space was set to larger than 15 Å in the *z* direction to surface isolation to prevent interaction between two neighboring slabs. All the atoms were allowed to relax for structural optimization calculations.

Gibbs free energies

The reaction activity in this work is estimated using the Gibbs Free Energy curves. For free energy change (ΔG) of elementary reaction can be defined as follows:

$$\Delta G = \Delta E_{DFT} + \Delta E_{ZPE} - T\Delta S$$

where ΔE_{DFT} is the reaction energy of the elementary reaction by DFT, *i.e.* the energy difference between the final and initial states. ΔE_{ZPE} and ΔS are the differences in zero-point energy and entropy change between the final and initial states, respectively.

References

(1) B. Hammer, L. B. Hansen, J. K. Nørskov, *Phys. Rev. B* **1999**, 59, 7413-7421;

(2) Y. K. Zhang, W. T. Yang, *Phys. Rev. B* **1998**, 80, 890;

(3) W. A. Brown, R. Kose, D. A. King, *Chem. Rev.* **1998,** 98, 797-831;

(4) K. Christmann, O. Schober, G. Ertl, *J. Chem Phys.* **1974**, 60, 4719-4724;

(5) G. Kresse, J. Furthmüller, *Comp. Mater. Sci.* **1996**, 6, 15;

(6) G. Kresse, J. Hafner, *Phys. Rev. B* **1993**, 47, 558;

(7) G. Kresse, J. Hafner, *Phys. Rev. B* **1994**, 49, 14251;

(8) G. Kresse, J. Furthmüller, *Phys. Rev. B* **1996**, 54, 11169;

(9) M. Dion, R. Rydberg, E. Schröder, D. C. Langreth, B. I. Lundqvist, *Phys. Rev. Lett.* **2004**, 92, 246401;

(10) J. Kliměs, D. R. Bowler, A. Michaelides, *J. Phys. Condens. Matter* **2010**, 22, 022201;

(11) R. Dronskowski, P. E. Bloechl, *J. Phys. Chem.* **1993**, 97, 8617;

(12) V. L. Deringer, A. L. Tchougréeff, R. Dronskowski, *J. Phys. Chem. A* **2011**, 115, 5461.

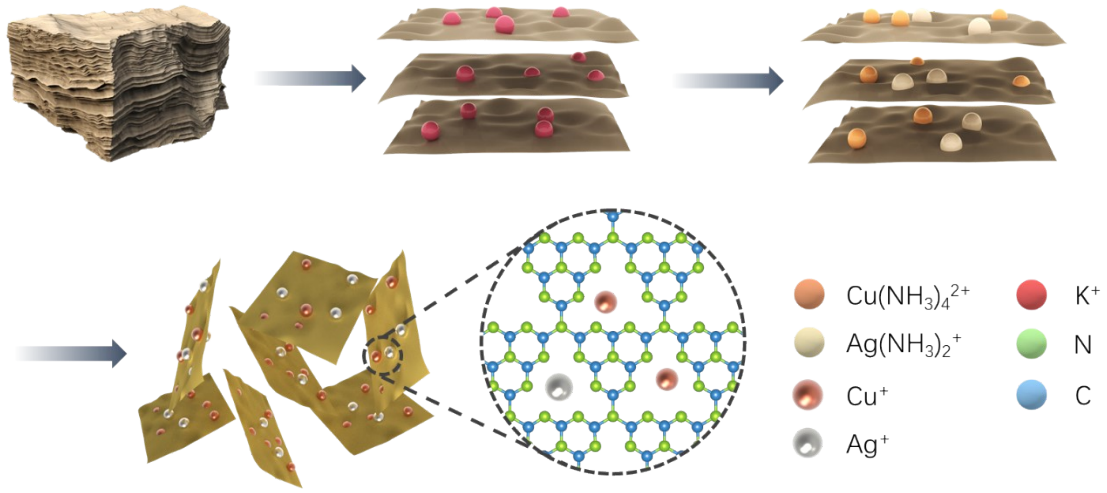

Figure S1. Schematic illustration of the preparation of AgCu-C_3N_4 SACs.

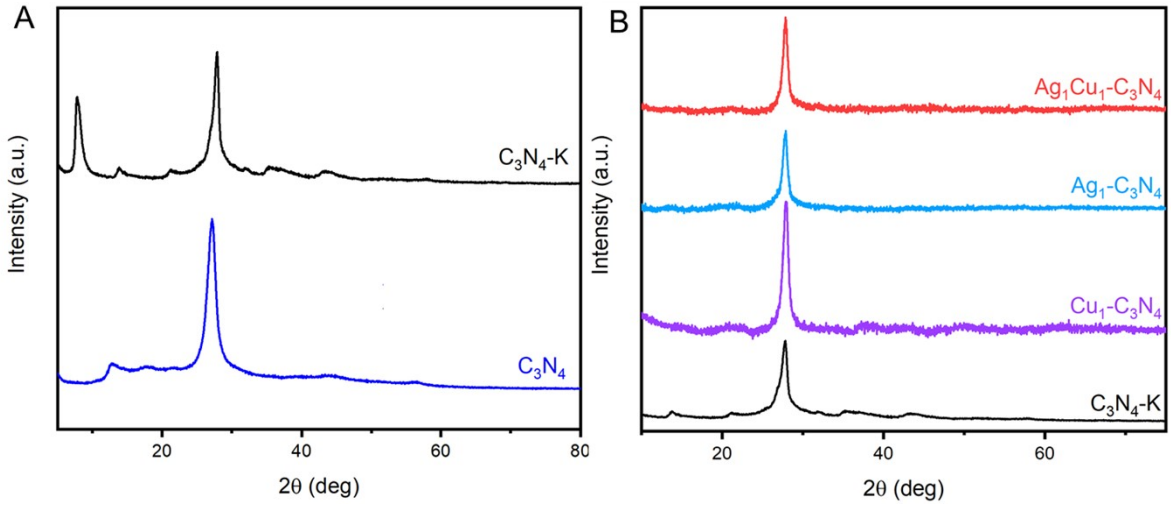

Figure S2. XRD patterns of (A) C_3N_4-K and *g*-C_3N_4 showing successful intercalation of K ions, and (B) AgCu-C_3N_4, Ag-C_3N_4, and Cu-C_3N_4 SACs compared with C_3N_4-K.

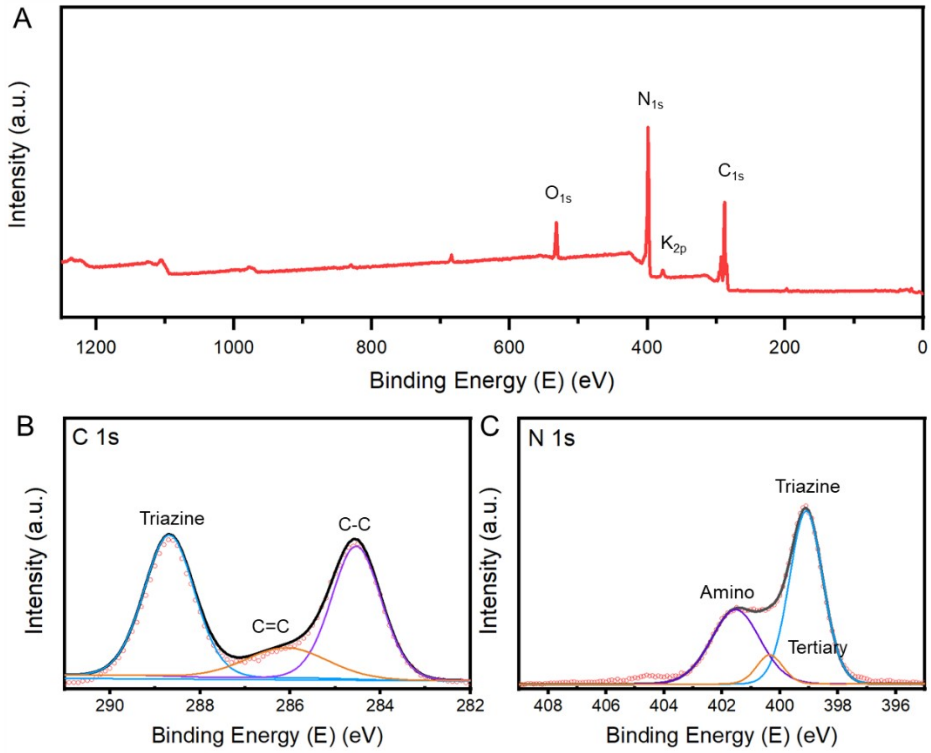

Figure S3. XPS spectra of C_3N_4–K: (A) survey; (B) C_{1s} and (C) N_{1s} spectra.

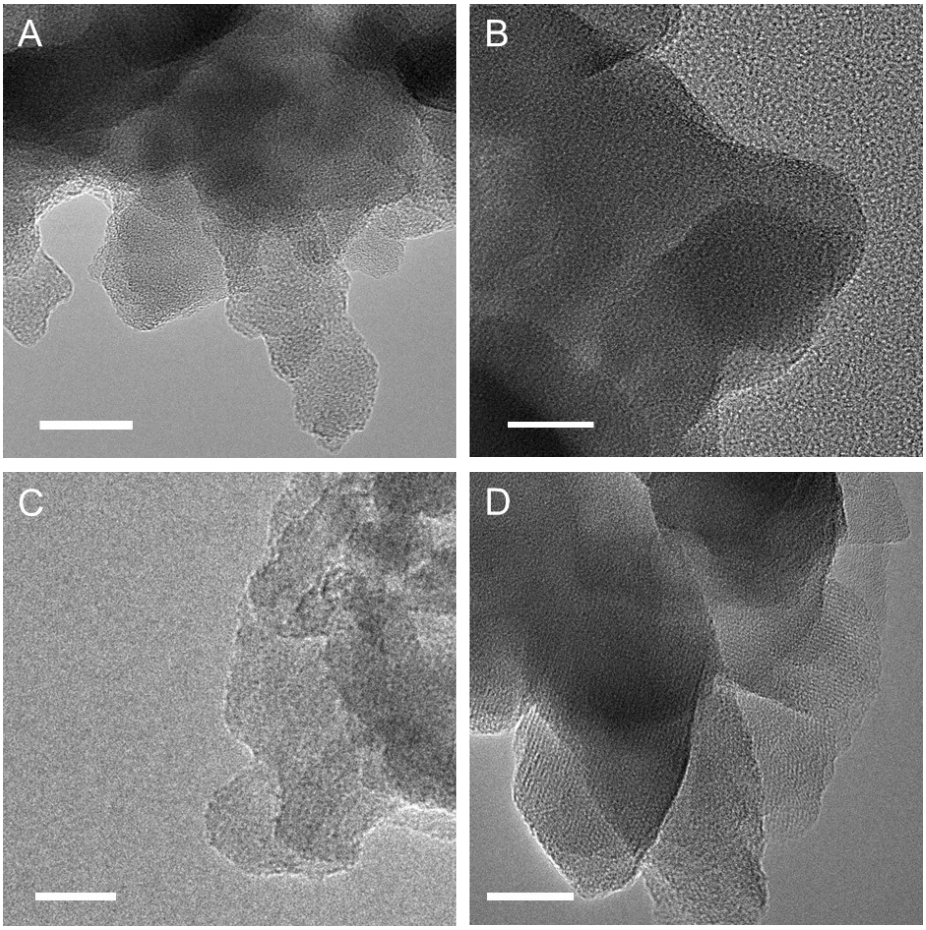

Figure S4. TEM images of as-prepared SACs and pristine support. (A) AgCu-C_3N_4, (B) Ag-C_3N_4 (C) Cu-C_3N_4 SACs, and (D) C_3N_4-K. Scale bar: (A-D) 20 nm.

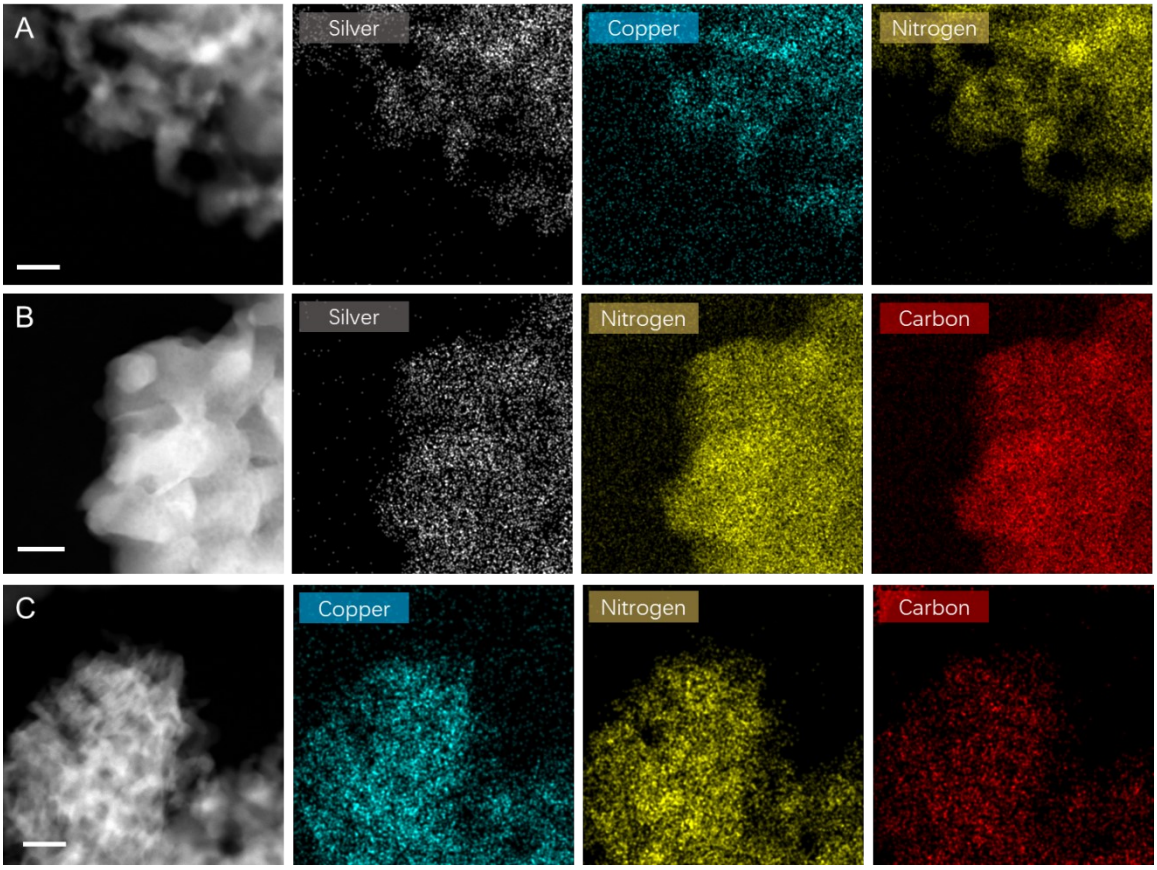

Figure S5. HAADF-STEM images and corresponding elemental mappings of (A) AgCu-C_3N_4, (B Ag-C_3N_4, and (C) Cu-C_3N_4 SACs. Elemental mappings: Ag (grey), Cu (cyan), N (yellow), and C (red). Scale bar: (A-C) 50 nm.

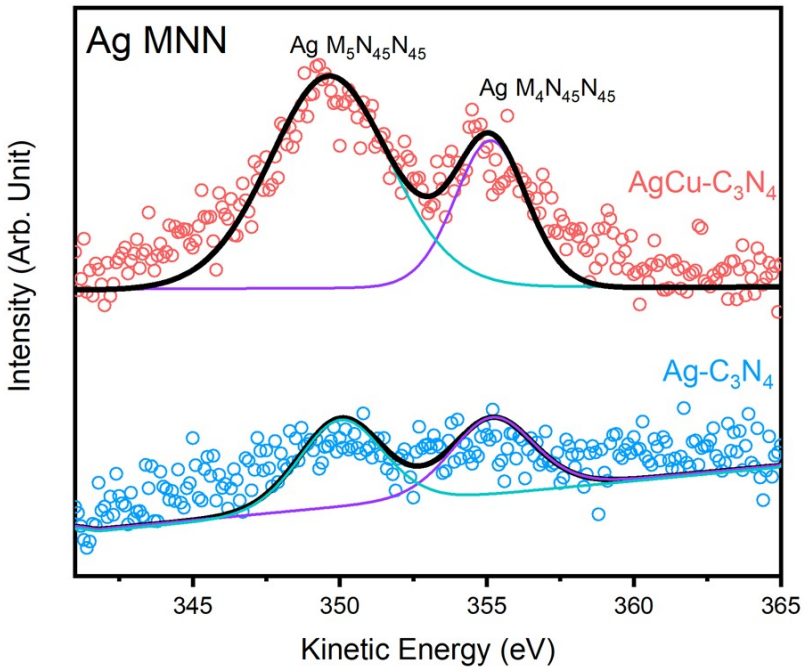

Figure S6. MNN Auger electron spectra of AgCu-C_3N_4 and Ag-C_3N_4.

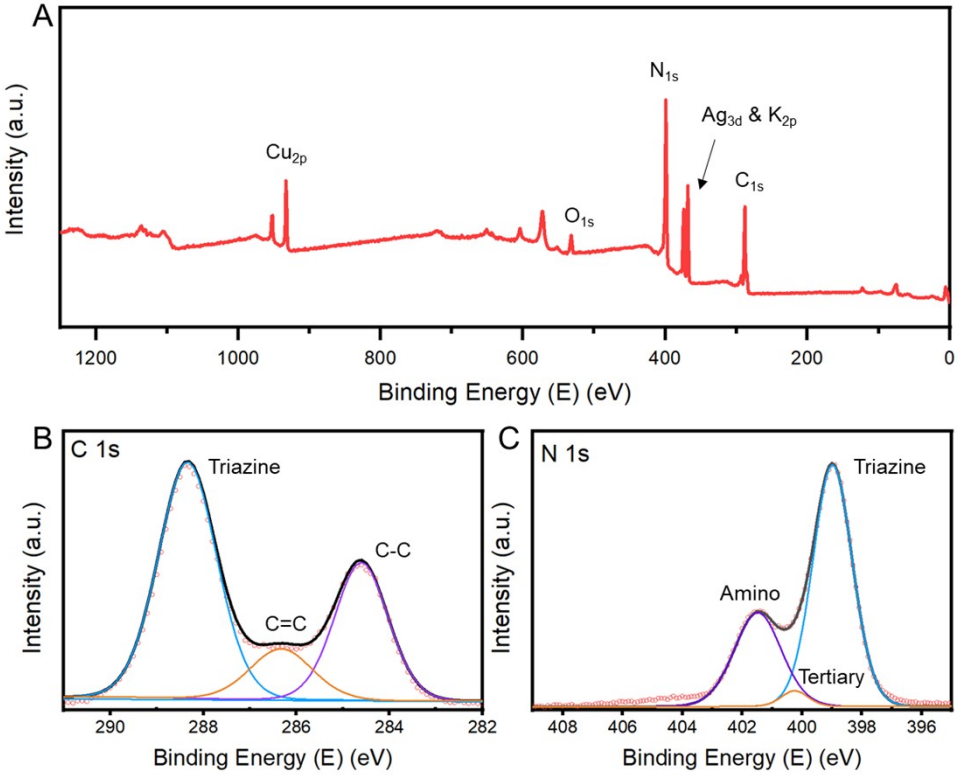

Figure S7. XPS spectra of AgCu-C_3N_4 SAC: (A) survey; (B) C_{1s} and (C) N_{1s} spectra.

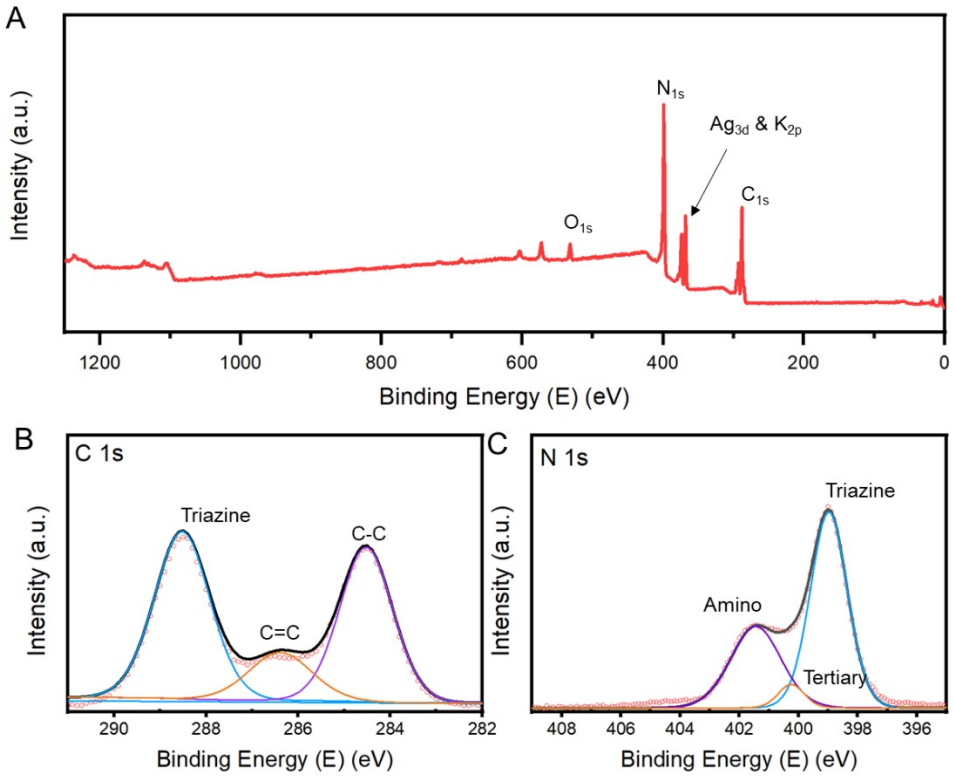

Figure S8. XPS spectra of Ag-C_3N_4 SAC: (A) survey; (B) C_{1s} and (C) N_{1s} spectra.

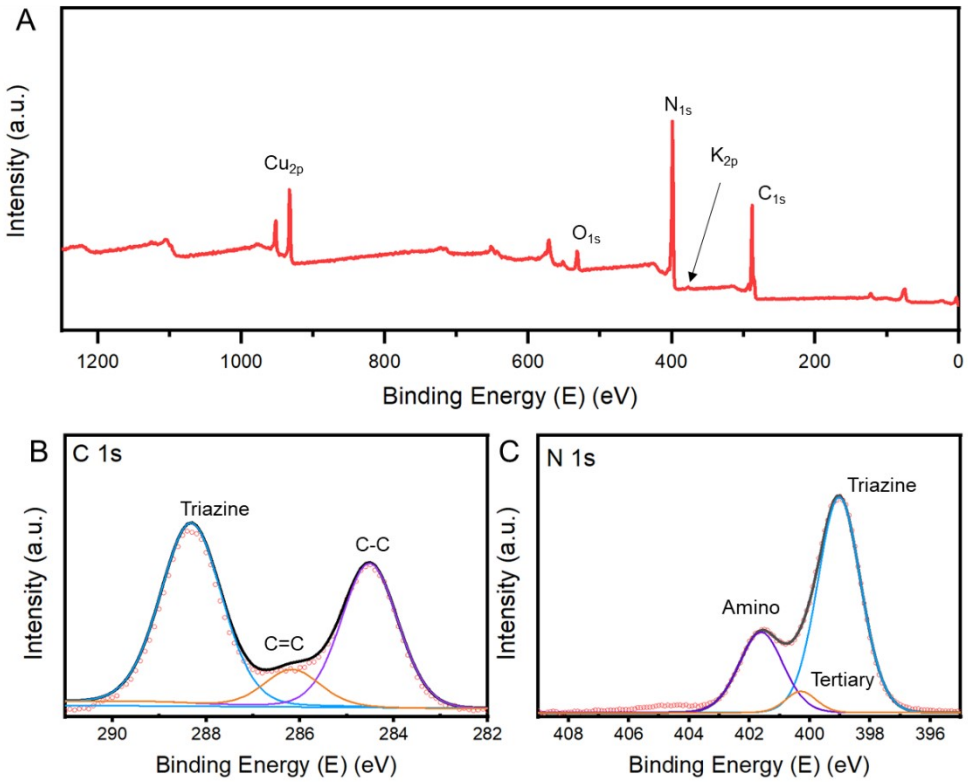

Figure S9. XPS spectra of Cu-C_3N_4 SAC: (A) survey; (B) C_{1s} and (C) N_{1s} spectra. Note that the peak labeled with * is associated with carbon paste during XPS sample preparation.

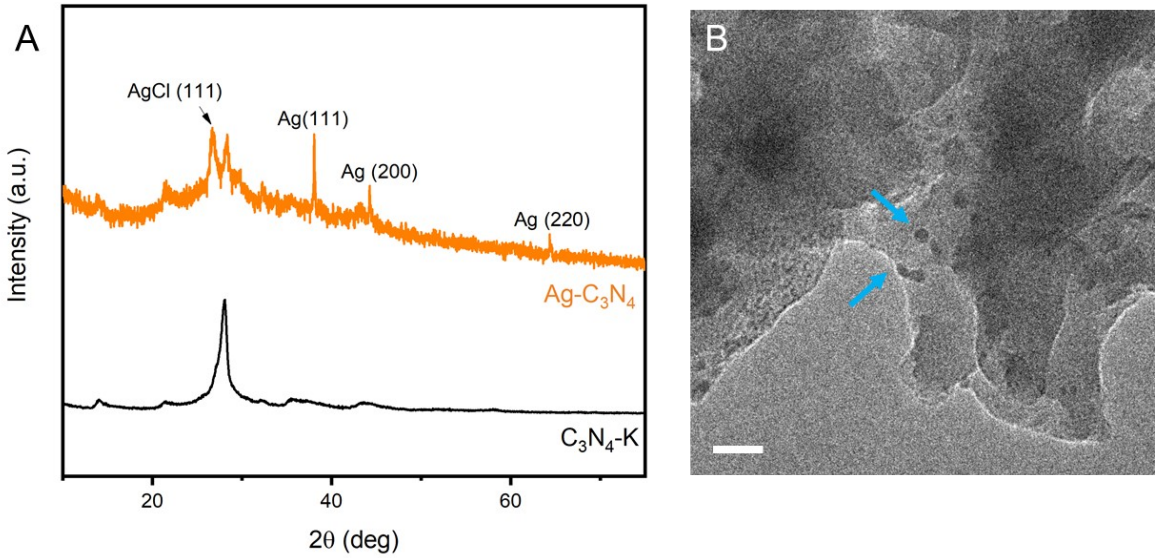

Figure S10. Characterization of 23 wt% Ag-C_3N_4. (A) XRD patterns of 23 wt% Ag-C_3N_4 and C_3N_4-K. (B) TEM image of 23 wt% Ag-C_3N_4. Ag particles can be identified as black dots under TEM. Scale bar: (A) 20 nm.

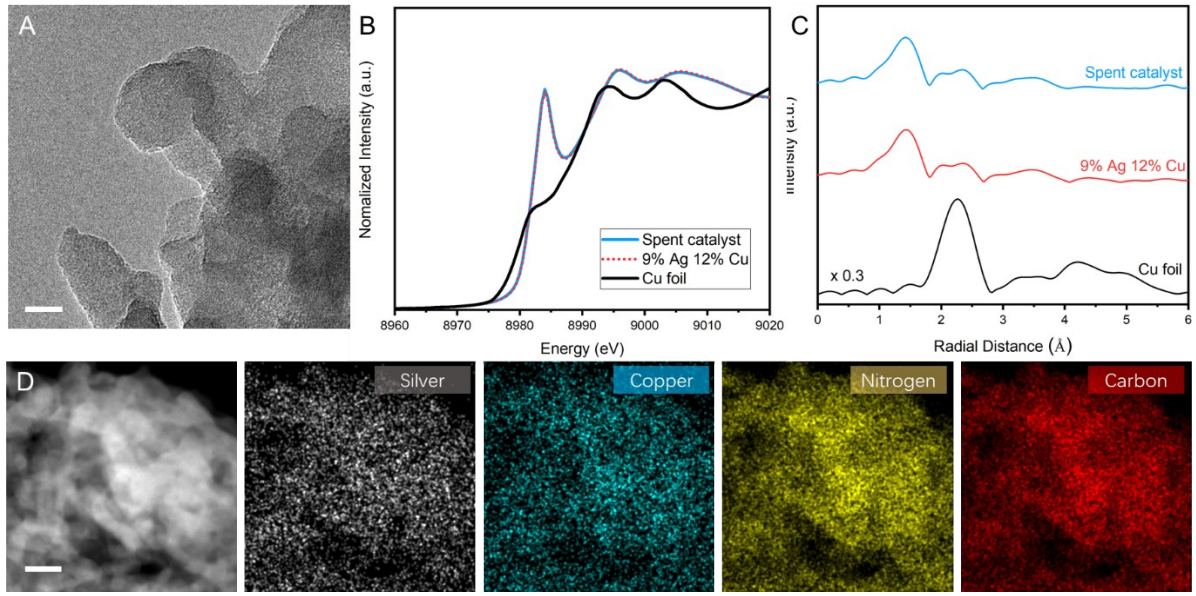

Figure S11. Characterization of spent AgCu-C_3N_4 SAC. (A)TEM image, which shows no particle aggregation; (B) Cu *K*-edge XANES spectra; (C) Cu FT-EXAFS spectra; and (D) HAADF-STEM images and corresponding elemental mappings of the spent AgCu-C_3N_4 SAC. Scale bar: (A) 20 nm; (D) 50 nm.

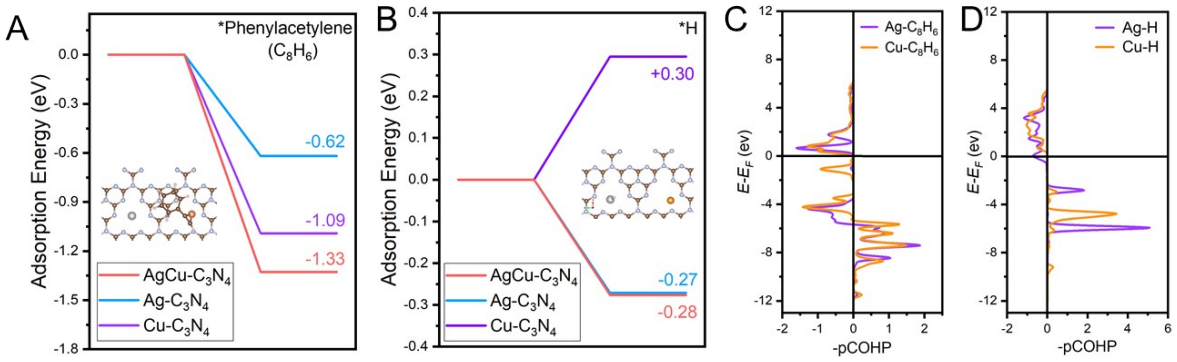

Figure S12. (A) Adsorption energy for phenylacetylene and (B) atomic H on AgCu-C_3N_4, Ag-C_3N_4, and Cu-C_3N_4 SACs. (C) The p-COHP curves for phenylacetylene and (D) atomic H adsorption on Ag and Cu site of AgCu-C_3N_4.

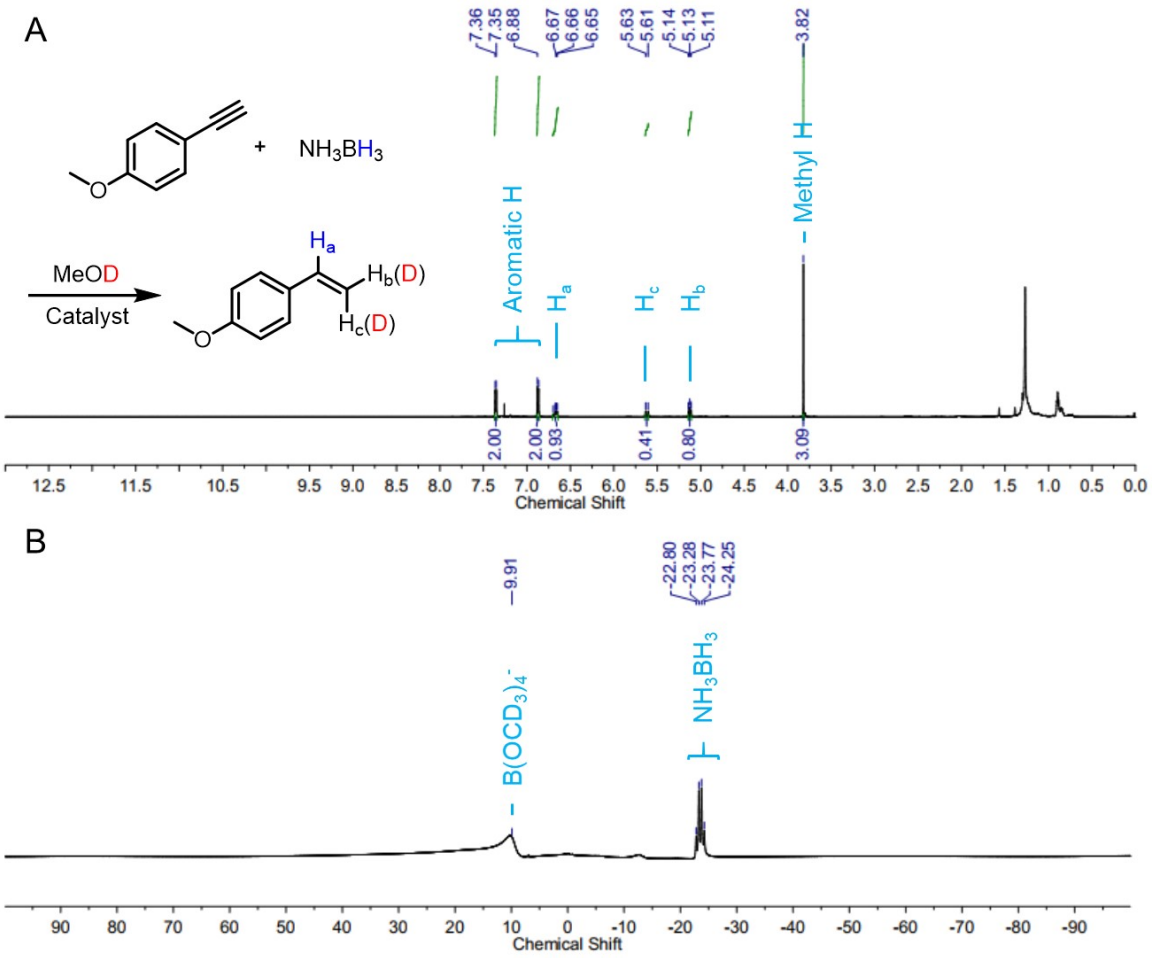

Figure S13. NMR spectrum for semi-hydrogenation product using MeOD as solvent. (A) ^{1}H NMR spectrum of alkene product and (B) ^{11}B NMR spectrum of reaction filtrate.

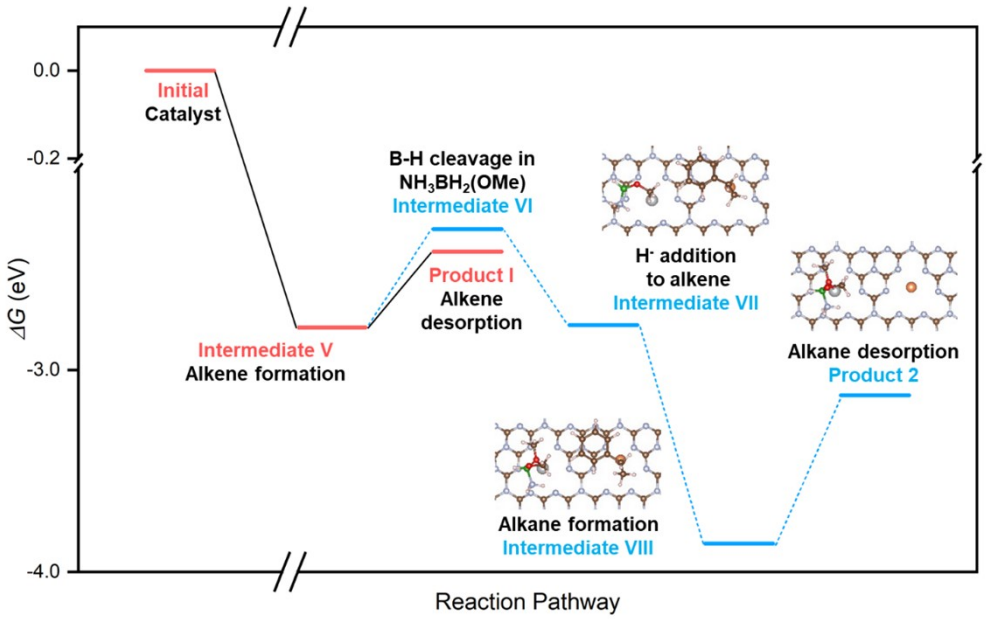

Figure S14. DFT-calculated energy pathway for fully hydrogenation of 4-ethynylanisole by NH_3BH_3. Steps of semi-hydrogenation to alkene has been omitted. Inset shows the optimized configuration of each intermediates adsorbed on AgCu-C_3N_4 catalyst. The color scheme used: silver for Ag, orange for Cu, brown for C; grey for N, green for B, red for O, and pink for H.

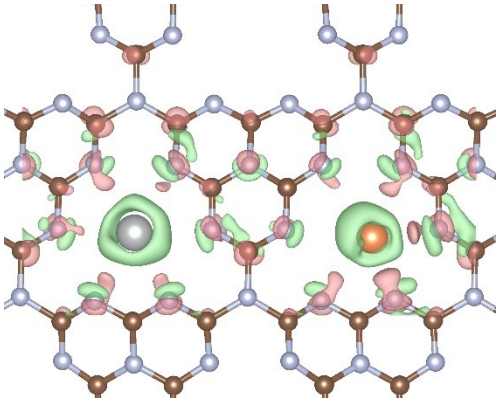

Figure S15. The charge density difference of AgCu-C3N4 model. The color scheme used: silver for Ag, orange for Cu, brown for C and grey for N. Green and pink regions in differential charge density represent electron accumulation and depletion, respectively.

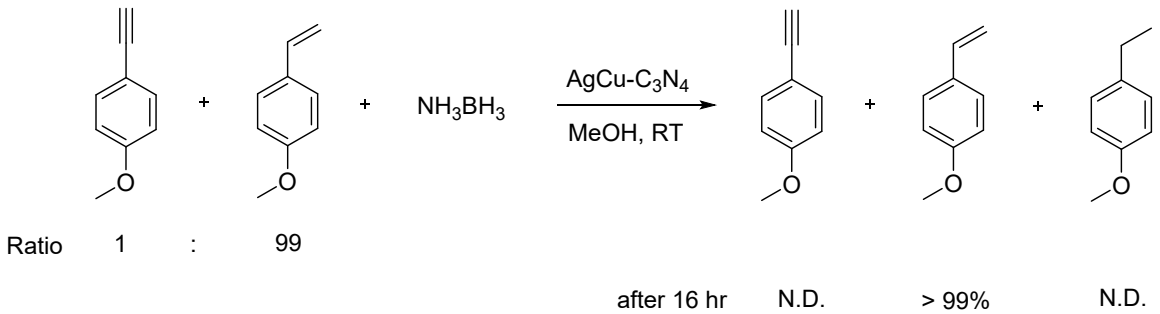

Figure S16. Demonstration of selective hydrogenation of alkyne to remove the trace amount of alkyne from alkene.

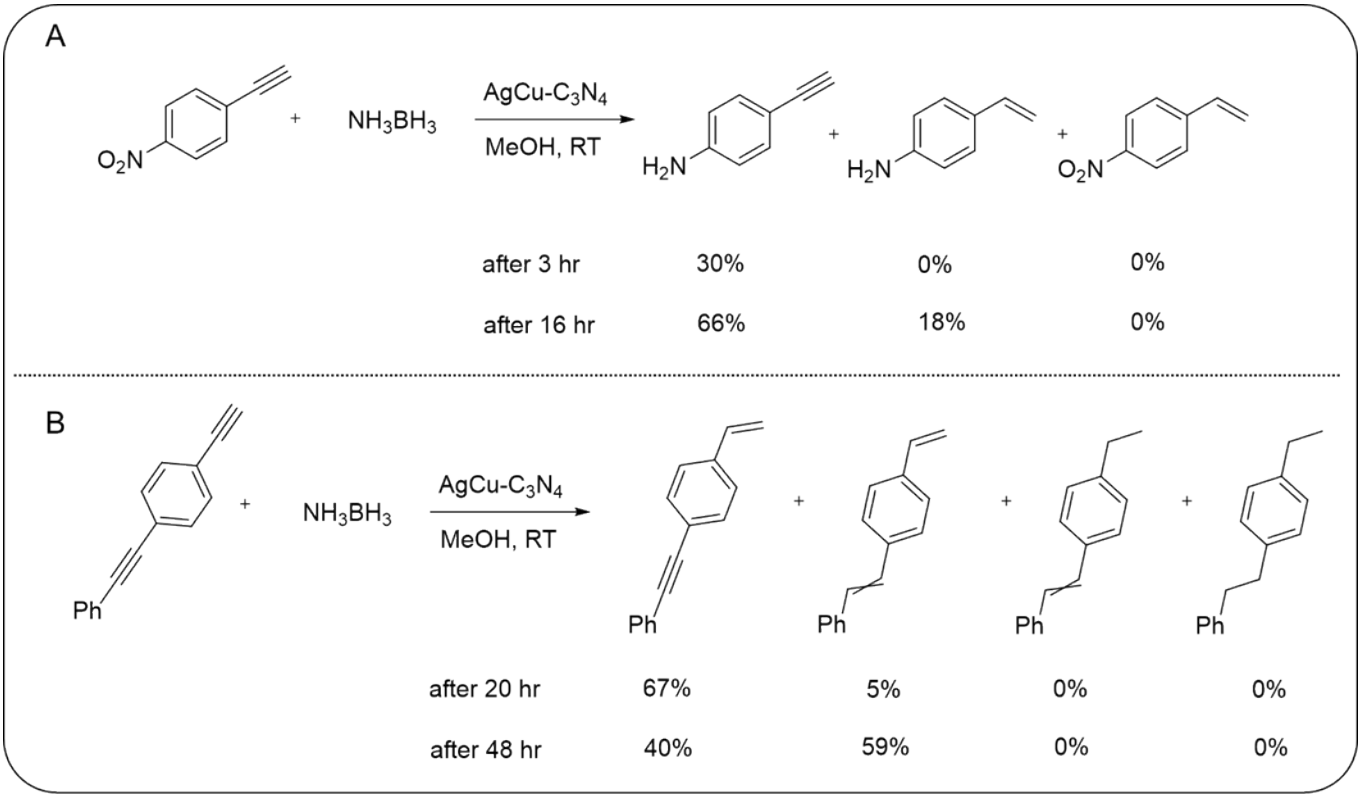

Figure S17. semi-hydrogenation of (A) *p*-nitrophenylacetylene and (B) 1-ethynyl-4-(phenylethynyl)benzene. For *p*-nitrophenylacetylene, Cu has a stronger affinity for the aryl nitro group than for the alkyne (*Nat Commun* **2022**, *13*, 2807), so reduction of the aryl nitro group occurs first, followed by the reduction of alkyne. In the case of 1-ethynyl-4-(phenylethynyl)benzene, the terminal alkyne is reduced first due to its less steric hindrance than the internal alkyne.

Table S1. Elementary composition of C_3N_4-based SACs.

Sample	ICP-OES Ag/wt%	ICP-OES Cu/wt%
$AgCu\text{-}C_3N_4$	9.2	12.0
$Ag\text{-}C_3N_4$	9.5	3.9
$Cu\text{-}C_3N_4$	21.4	1.5

Table S2. The elementary composition of AgCu-C_3N_4 SACs for metal loading dependent catalytic performance study in **Figure 3C**.

Sample	ICP-OES Ag/wt%	ICP-OES Cu/wt%	***2a*** yield
1	4.0	9.2	5%
2	3.0	11.9	27%
3	8.8	12.0	99%
4	15.7	8.5	99%
5	14.4	3.9	99%
6	14.6	1.5	99%
7	7.0	5.0	33%
8	6.7	2.5	25%
9	3.2	2	1%

Table S3. Results of the EXAFS fitting of various catalysts.

	Bonding	N	R (Å)	σ^2 (Å^2)	ΔE_0 (eV)	R-factor
AgCu-C_3N_4	Cu-N	2.8 ± 0.5	1.89	0.006	4.46	0.005
	Ag-N	2.5± 0.9	2.21	0.008	-0.153	0.01
Ag-C_3N_4	Ag-N	2.9 ± 0.5	2.21	0.007	1.83	0.01
Cu-C_3N_4	Cu-N	3.4 ± 0.2	1.91	0.007	3.78	0.002
Spent catalyst	Cu-N	3.1 ± 0.5	1.89	0.005	4.03	0.006
Ag_2O	Ag-O	2.0	2.05	0.003	5.41	0.002
Ag foil	Ag-Ag	12.0	2.86	0.011	1.03	0.008
Cu foil	Cu-Cu	12.0	2.54	0.008	3.51	0.002

Table S4. Reaction condition screening for semi-hydrogenation of 4-ethynylanisole[a]

Entry	Reductant	Solvent	Temperature	Reaction Time	Yield (%)
1	NH_3BH_3	MeOH	R.T	20 hr	99
2	NH_3BH_3	Ethyl acetate	R.T	20 hr	0
3	NH_3BH_3	Dichloromethane	R.T	20 hr	0
4	NH_3BH_3	Diethyl ether	R.T	20 hr	0
5	NH_3BH_3	THF (anhydrous)	R.T	20 hr	0
6	NH_3BH_3	THF/MeOH = 10:1	R.T	20 hr	45
8	NH_3BH_3	EtOH	R.T	20 hr	28
9	NH_3BH_3	iPr-OH	R.T	20 hr	18
10	NH_3BH_3	H_2O	R.T	20 hr	77
11[b]	H_2 (1 atm)	MeOH	R.T	20 hr	0
12	NH_3BH_3	MeOH	45 ℃	10 hr	99
13	NH_3BH_3	MeOH	60 ℃	2 hr	99

[a] Condition: 0.1 mmol of 4-ethynylanisole (13 μL), 0.5 mmol of NH_3BH_3 (15.0 mg), 1 mL of solvent, AgCu-C_3N_4 SAC (3mg), room temperature, 24 h, under ambient condition. The yield of 4-vinylanisole was determined by GC-MS; [b] H_2 balloon was used without adding NH_3BH_3.

Table S5. Performance tracker for SAC catalysed semi-hydrogenation of alkynes.

Catalyst	Solvent	Reducing agent	Temperature	Alkene selectivity	Reference
AgCu-C_3N_4	MeOH	NH_3BH_3	RT to 60 ℃	> 99%	This work
Pd_1/BP	MeOH	NH_3BH_3	80 ℃	> 90%	*Adv. Mater.* **2021**, 33, 2008471
Cu_1/CN/Al_2O_3	MeOH	NH_3BH_3	70 ℃	98%	*Chem. Sci.* **2021**, 12, 14599
PdNP@Ni_1-γ-Al_2O_3	EtOH	H_2 (1atm)	RT	> 99%	*ACS Catal.* **2022**, 12, 24, 14846
Pd_1/ZIF-8	Ethyl Acetate	H_2 (1atm)	120 ℃	100%	*Nano Res.* **2023**, 16, 8003
Pd_1/Ni@G	EtOH	H_2 (2 bar)	30 ℃	93%	*Adv. Mater.* **2022**, 34, 2110455
Pt_1–Sn_1/N–C	MeOH	H_2 (10 atm)	50 ℃	> 97%	*Nat Commun* **2019**, 10, 3663
Pd_1@Cu-SiW	Gas-phase reaction	H_2	120 ℃	93%	*Angew. Chem. Int. Ed.* **2021**, 60, 22522
Pd_1/N-graphene	Gas-phase reaction	H_2	125 ℃	93.5%	*Adv. Mater.* **2019**, 31, 1900509
Pd_1Cu_1/ND@G	Gas-phase reaction	H_2	110 ℃	92%	*J. Am. Chem. Soc.* **2022**, 144, 40, 18485
Pd_1/CeO_2	Gas-phase reaction	H_2	160 ℃	85%	*Nano Res.* **2022**, 15, 10037

---

^{1}H NMR of organic compounds.

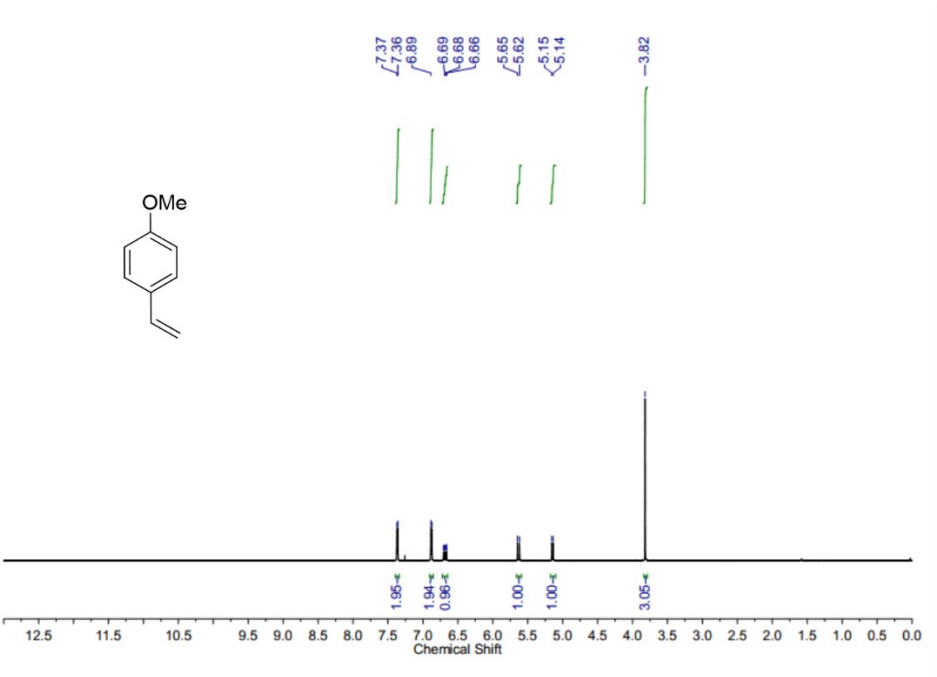

1-methoxy-4-vinylbenzene (*2a*). ^{1}H NMR (600 MHz, $CDCl_3$) δ = 7.37-7.36 (d, 2H), 6.89 (s, 2H), 6.69-6.66 (m, 1H), 5.65-5.62 (d, 1H), 5.15-5.14 (d, 1H), 3.82 (s, 3H).

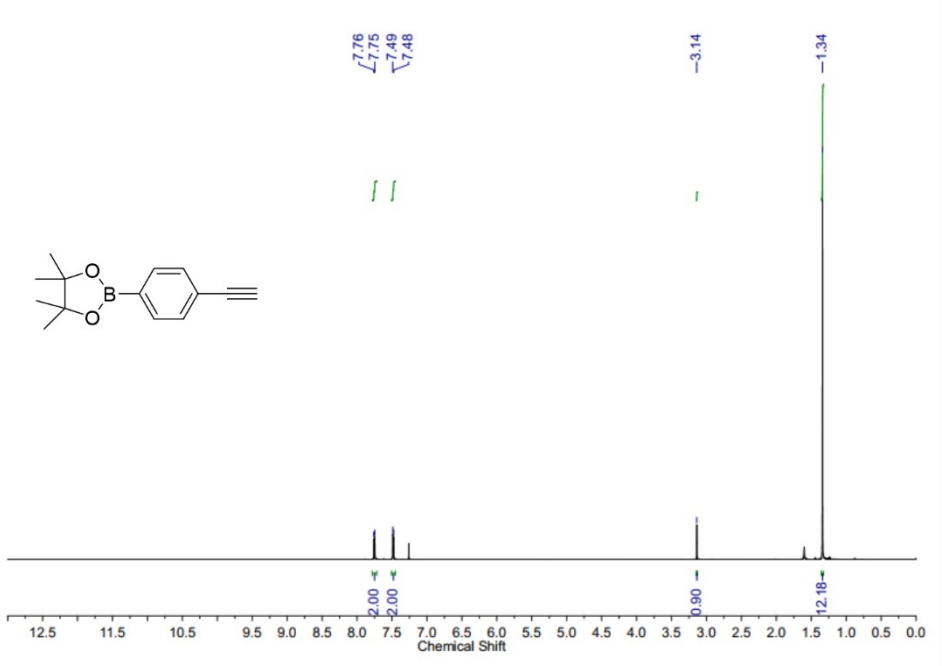

2-(4-ethynylphenyl)-4,4,5,5-tetramethyl-1,3,2-dioxaborolane (*1b*). ^{1}H NMR (600 MHz, $CDCl_3$) δ = 7.76-7.75 (d, 2H), 7.49-7.48 (d, 2H), 3.14 (s, 1H), 1.34 (s, 12H).

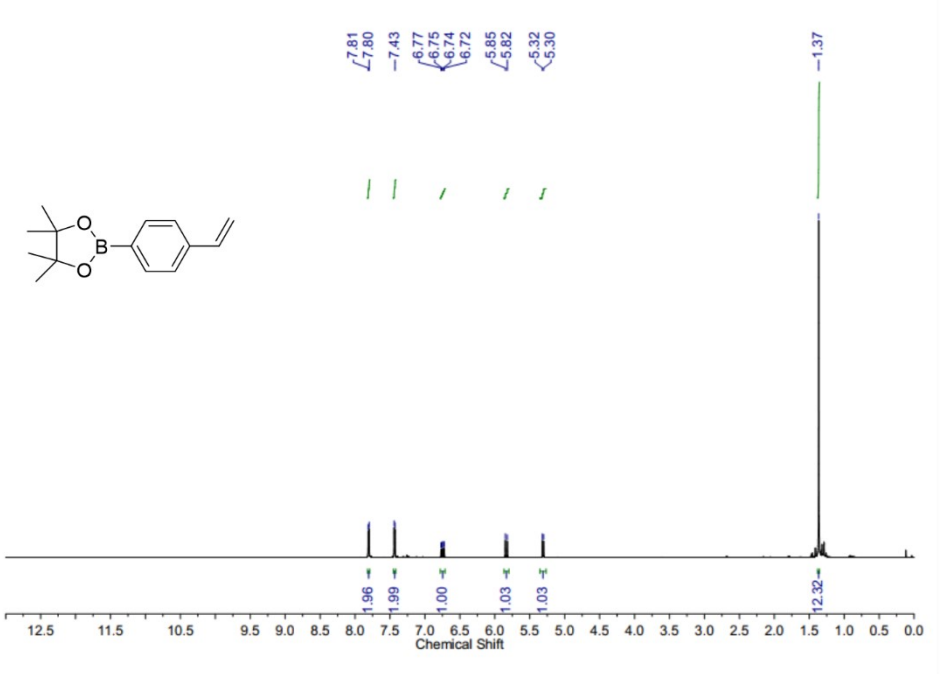

4,4,5,5-tetramethyl-2-(4-vinylphenyl)-1,3,2-dioxaborolane (*2b*). ^{1}H NMR (600 MHz, $CDCl_3$) δ = 7.81-7.80 (d, 2H), 7.44-7.43 (d, 2H), 6.77-6.72 (m, 1H), 5.85-5.82 (d, 1H), 5.32-5.30 (d, 1H), 1.37 (s, 12H).

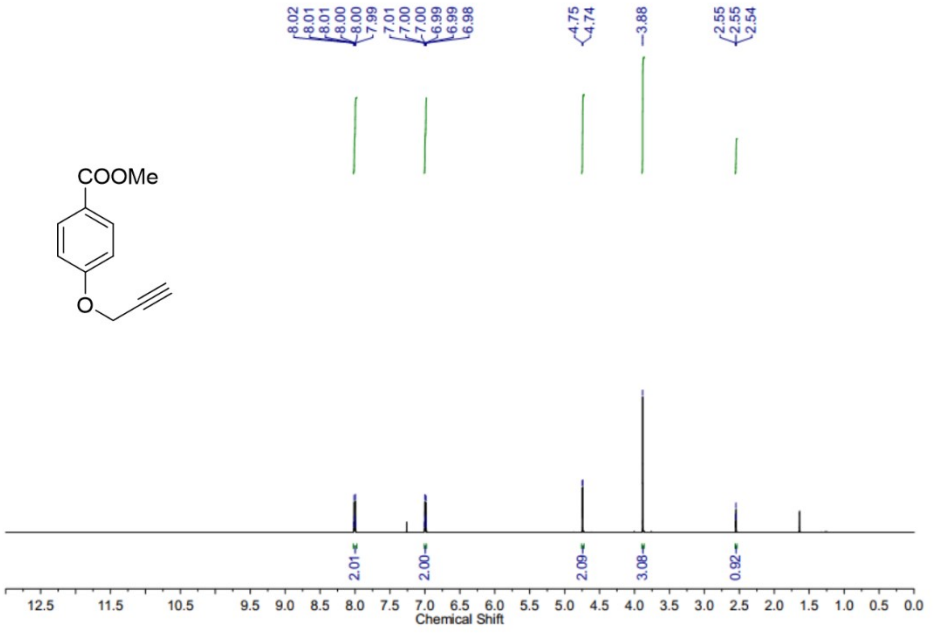

Methyl 4-(ethynyloxy)benzoate (*1c*). ^{1}H NMR (600 MHz, $CDCl_3$) δ = 8.02-7.99 (m, 2H), 7.01-6.98 (m, 2H), 4.75-4.74 (d, 2H), 3.88 (s, 3H), 2.55-2.54 (t, 1H).

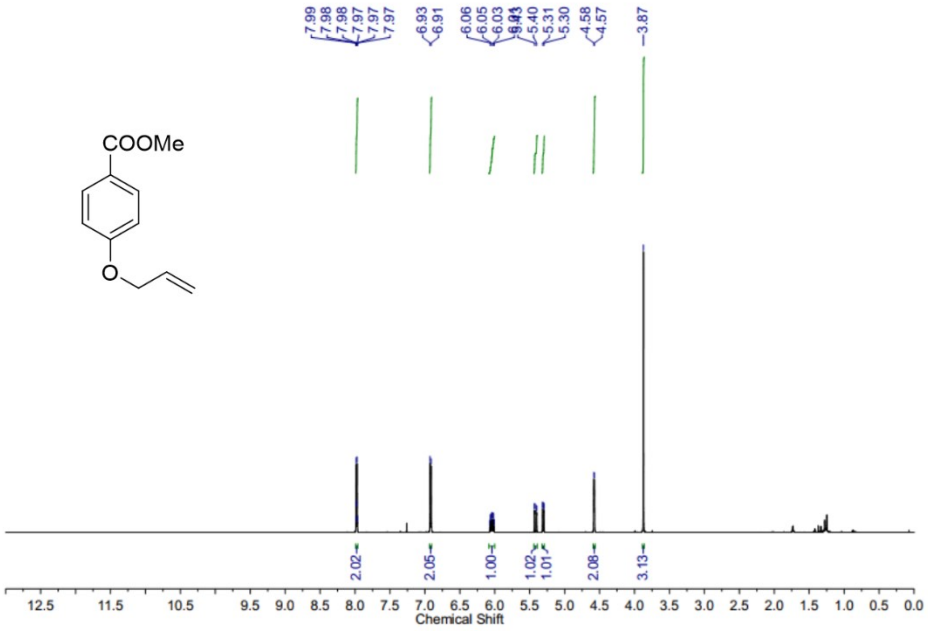

Methyl 4-(vinyloxy)benzoate (*2c*). ^{1}H NMR (600 MHz, $CDCl_3$) δ = 7.99-7.97 (m, 2H), 6.93-6.91 (d, 2H), 6.07-6.01 (m, 1H), 5.43-5.40 (m, 1H), 5.32-5.30 (m, 1H), 4.58-4.57 (d, 2H), 3.87 (s, 3H).

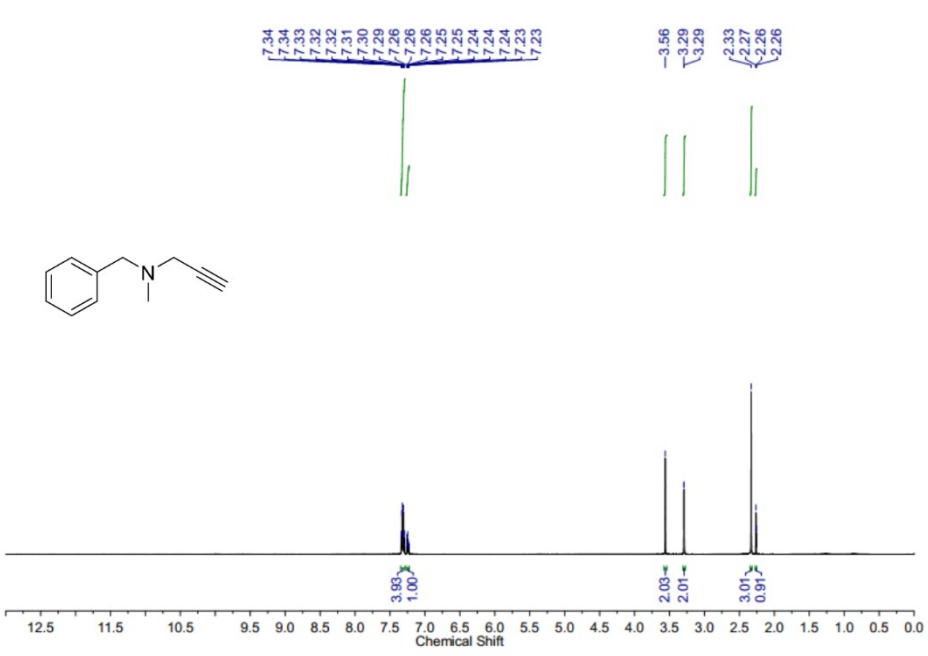

N-benzyl-N-methylprop-2-yn-1-amine (*1d*). ^{1}H NMR (600 MHz, $CDCl_3$) δ = 7.34-7.29 (m, 4H), 7.26-7.23 (m, 1H), 3.56 (s, 2H), 3.29 (d, 2H), 2.33 (s, 3H), 2.27-2.26 (t, 1H).

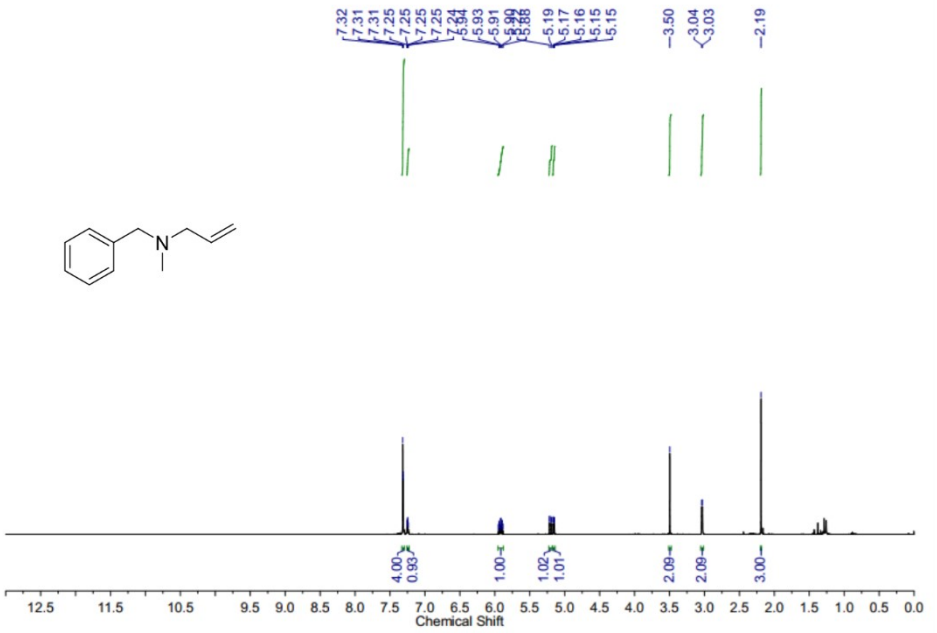

N-benzyl-N-methylprop-2-en-1-amine (*2d*). ^{1}H NMR (600 MHz, $CDCl_3$) δ = 7.32-7.31 (m, 4H), 7.25-7.24 (m, 1H), 5.95-5.88 (m, 1H), 5.22-5.19 (m, 1H), 5.17-5.15 (m, 1H), 3.50 (s, 2H), 3.04-3.03 (d, 2H), 2.19 (s, 3H).

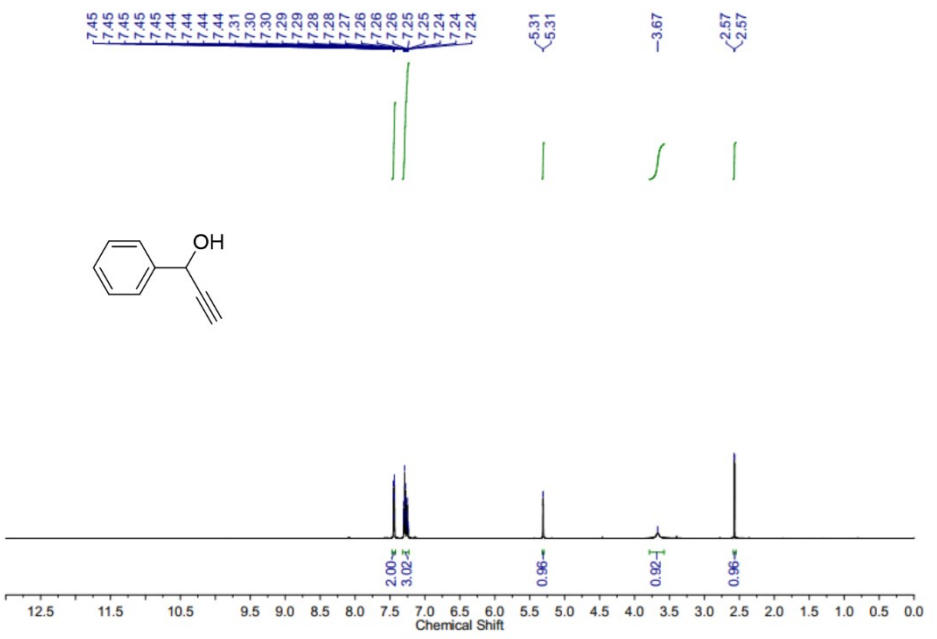

1-phenylprop-2-yn-1-ol (*1e*). ^{1}H NMR (600 MHz, $CDCl_3$) δ = 7.45-7.44 (m, 2H), 7.31-7.24 (m, 3H), 5.31 (d, 1H), 3.67 (s, 1H), 2.57 (d, 1H).

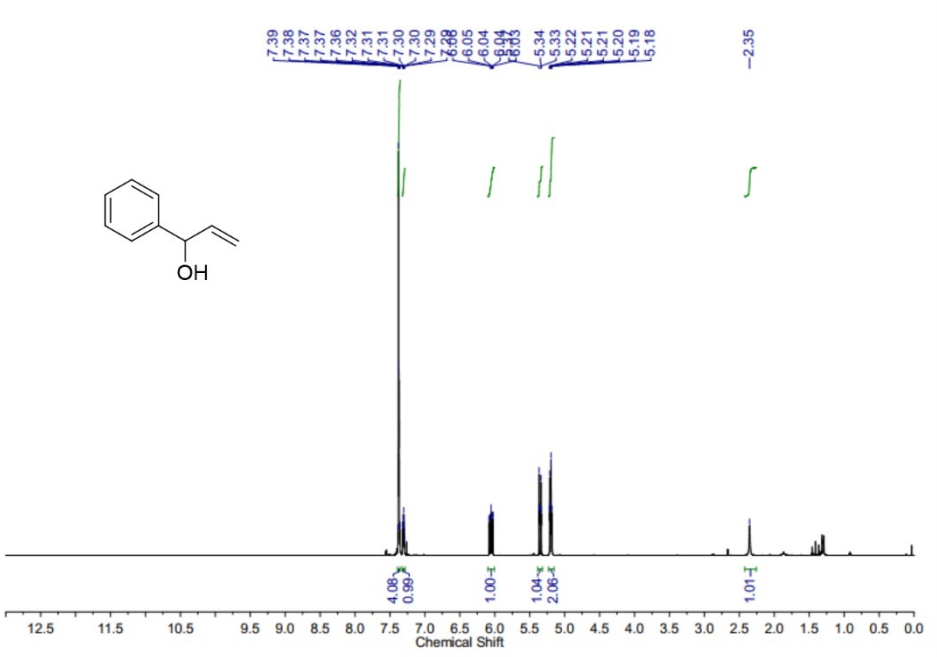

1-phenylprop-2-en-1-ol (*2e*). ^{1}H NMR (600 MHz, $CDCl_3$) δ = 7.39-7.36 (m, 4H), 7.32-7.29 (m, 1H), 6.08-6.03 (m, 1H), 5.37-5.33 (m, 1H), 5.22-5.18 (m, 1H), 2.35 (s, 1H).

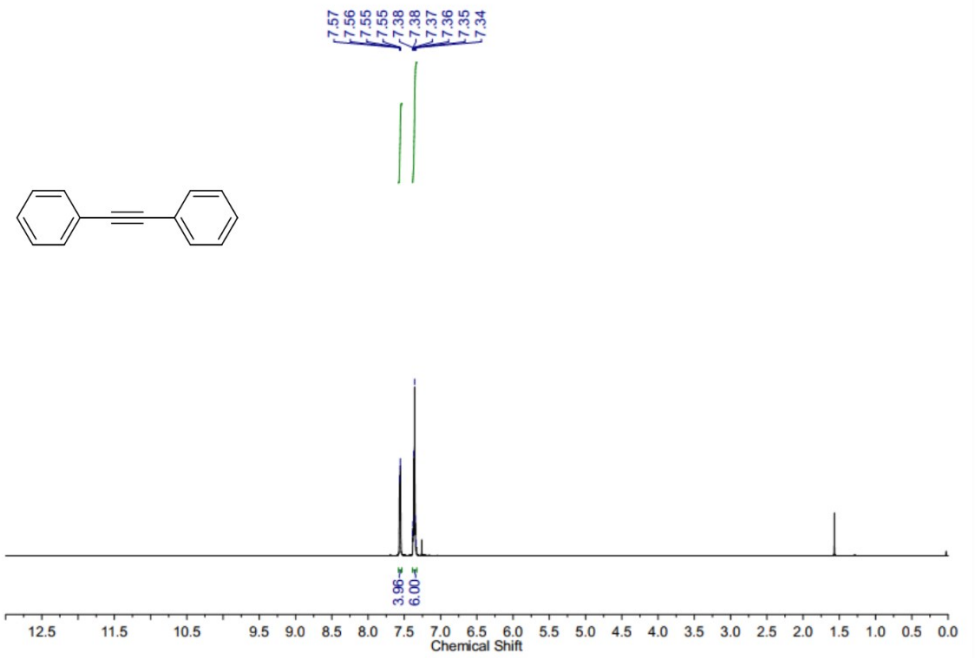

1,2-diphenylethyne (*1f*). ^{1}H NMR (600 MHz, $CDCl_3$) δ = 7.57-7.38 (m, 4H), 7.38-7.34 (m, 6H).

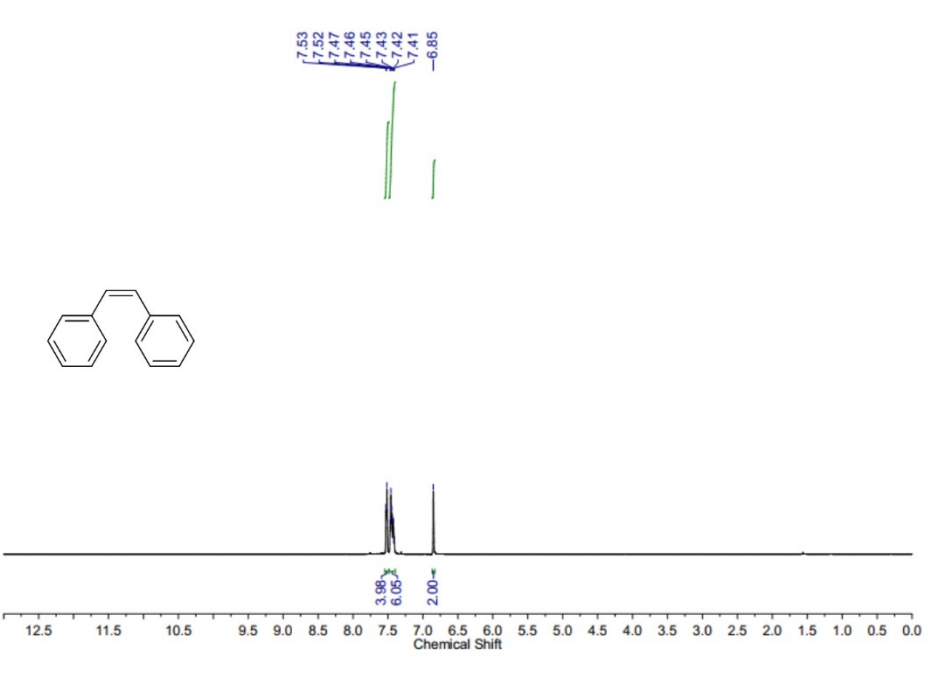

(*Z*)-1,2-diphenylethene (*2f-cis*). ^{1}H NMR (600 MHz, $CDCl_3$) δ = 7.53-7.52 (d, 4H), 7.47-7.41 (m, 6H), 6.85 (s, 2H).

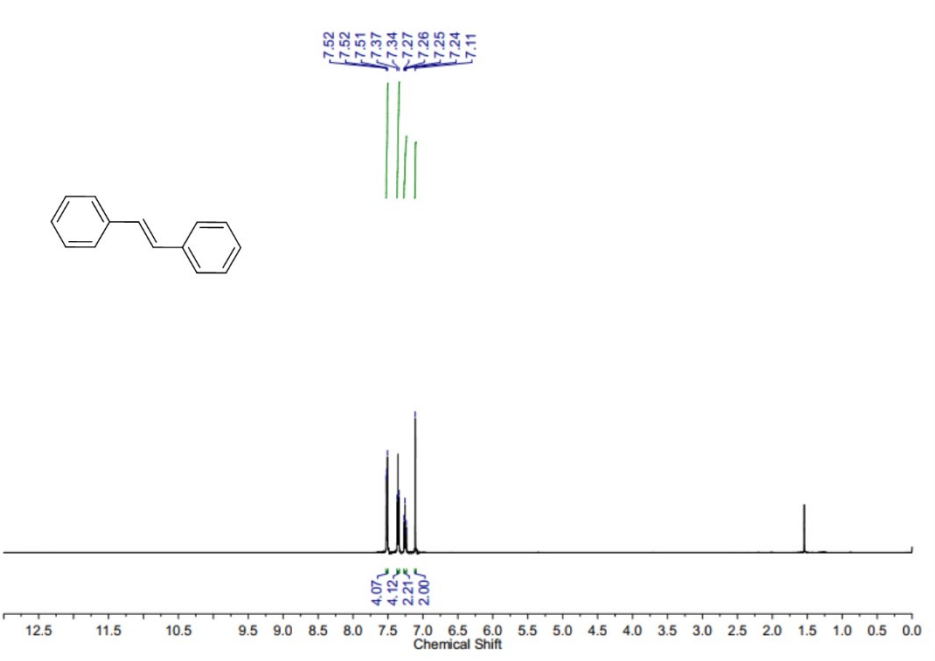

(*E*)-1,2-diphenylethene (*2f-trans*). ^{1}H NMR (600 MHz, $CDCl_3$) δ = 7.52-7.51 (m, 4H), 7.37-7.34 (m, 4H), 7.27-7.24 (m, 2H), 7.11 (s, 2H).

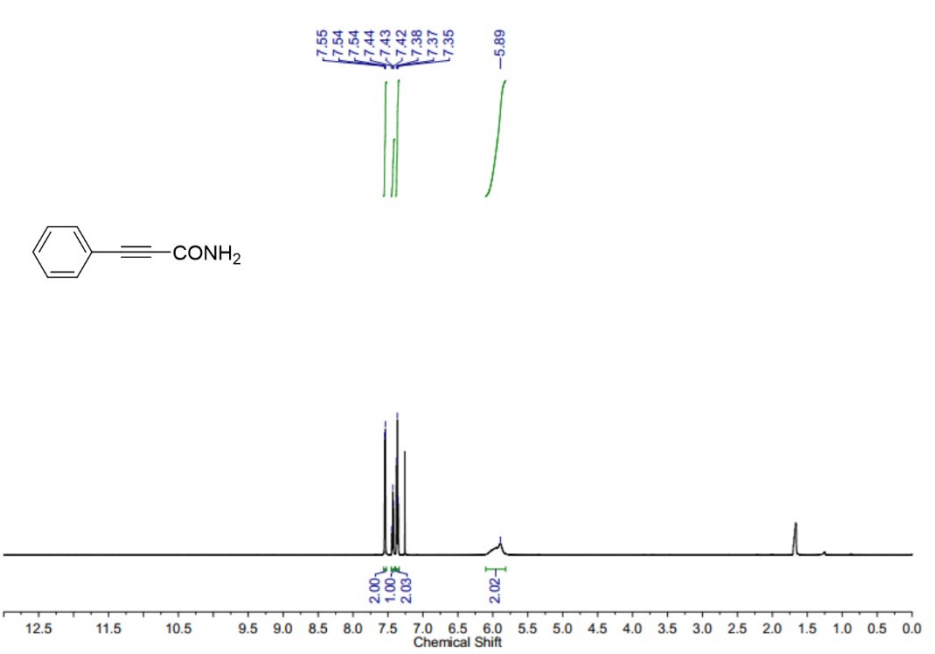

3-phenylpropiolamide (*1g*). ^{1}H NMR (600 MHz, $CDCl_3$) δ = 7.55-7.54 (m, 2H) 7.44-7.42 (t, 1H), 7.38-7.35 (t, 2H), 5.89 (s, 2H).

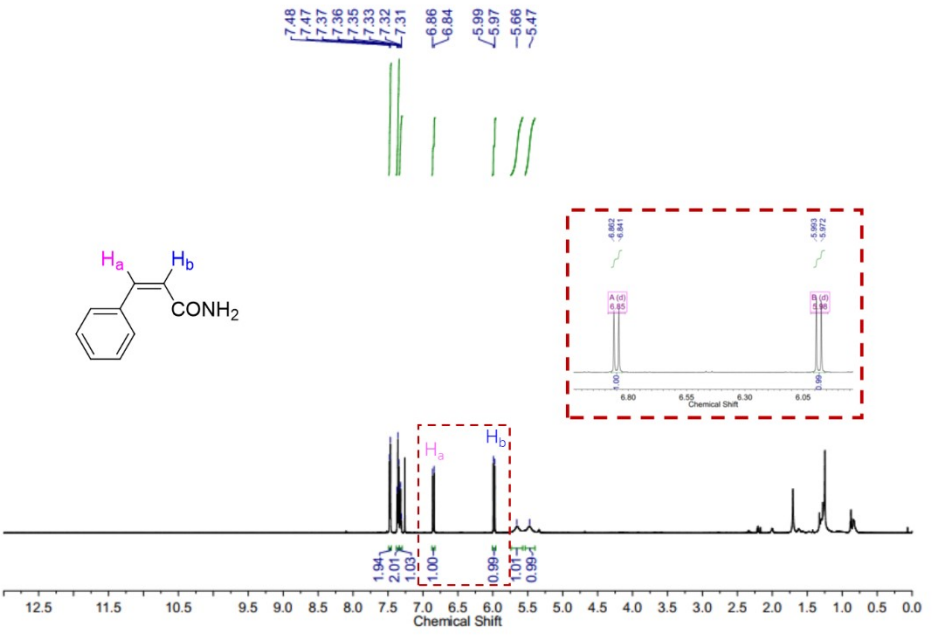

(*Z*)-3-phenylacrylamide (*2g-cis*). ^{1}H NMR (600 MHz, $CDCl_3$) δ = 7.48-7.47 (d, 2H), 7.37-7.35 (m, 2H), 7.33-7.31 (m, 1H), 6.86-6.84 (d, 1H, *J* = 12.6 Hz), 5.99-5.97 (d, 1H, *J* = 12.6 Hz), 5.66 (s, 1H), 5.47 (s, 1H).

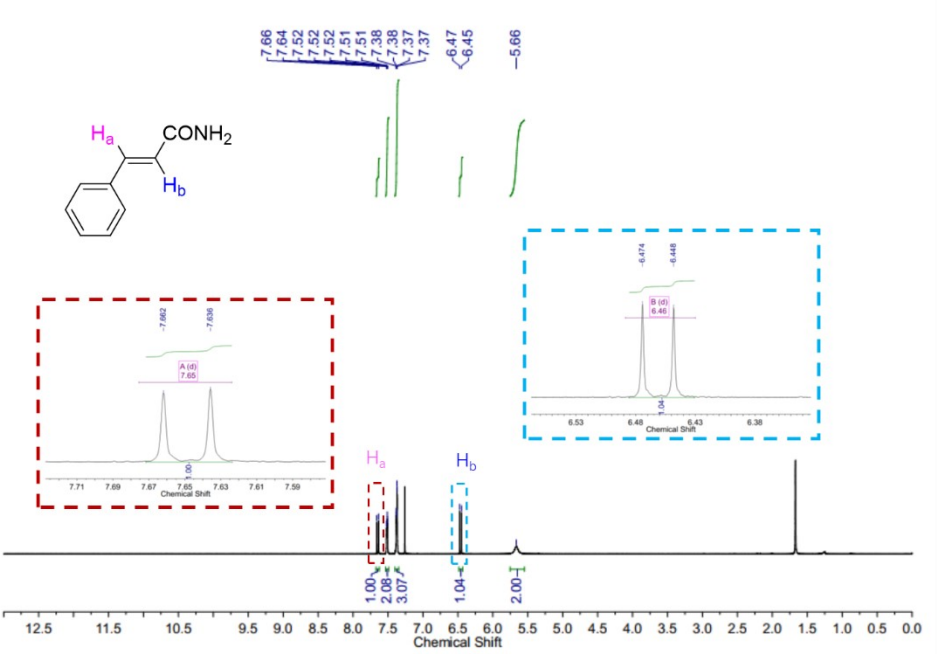

(*E*)-3-phenylacrylamide (*2g-trans*). ^{1}H NMR (600 MHz, $CDCl_3$) δ = 7.66-7.64 (d, 1H, *J* = 15.6 Hz), 7.52-7.51 (m, 2H), 7.38-7.37 (m, 3H), 6.47-6.45 (d, 1H, *J* = 15.6 Hz), 5.66 (s, 2H).